

# Self-Organization in Networks of Spiking Neurons

Dorel M. Sala, Krzysztof J. Cios and John T. Wall\*

University of Toledo and Medical College of Ohio\*, Toledo, Ohio, U.S.A.

## Abstract

Traditionally artificial neural network design was based on average firing rate model of a biological neuron. In this paper we briefly review approaches based on single action potentials. Then we describe a self-organizing neural network based on a spiking neuron model. We show how this network of laterally connected spiking neurons self-organizes into a topological map in response to external stimulation. Two unsupervised, activity-dependent, instantaneous learning rules for adjusting the synaptic efficacies are introduced and analyzed in the paper. The first rule is based on the postsynaptic contribution of the presynaptic neuron, while the second, called *temporal correlation rule* is based only on the time difference between the pre- and postsynaptic neuron spikes. Interestingly applying either of the two learning rules results in a well-segregated map, where the afferent connections from non-active input neurons die-off and the lateral connections gradually restrict themselves into one of the regions of the formed map. We also draw an analogy between our temporal correlation learning rule and Kohonen's SOM learning rule.

**Keywords:** Spiking neurons, selforganization, and synaptic plasticity

## 1 Introduction

In choosing a type of artificial Neural Network (NN) one has to answer few basic questions. How close the neuron model must be to its biological counterpart? To what extent simplifying assumptions can be made? What is the goal of modeling?

In this paper we answer some of these questions by focusing on time and its role in information processing. In this respect we first have to consider how much information is conveyed by an action potential. For example, each action potential could represent a single bit of information, or one bit of information can be spread over many action potentials so that information per pulse is very small [9].

The first recordings of a sensory neuron activity showed that the spike frequency of a neuron is related to the intensity of the stimulus [16]. From that observation to describing the neuron activity by the firing rate was just a natural step. If one takes into account other phenomena, like the effect of noise, spontaneously generated spike, etc. this approach seems well justified.

Recent biological evidence [3, 7, 15] has shown that some biological neural systems use exact spike times or the length of interspike intervals to encode information. In many situations fast reaction of the system is required [17] so that there is no time for temporal averaging. This leaves single spikes, synchronized activity in populations of neurons [4, 5], and other still unknown mechanisms as alternatives to explore.

The time aspect has been usually disregarded in the standard approach to artificial neural networks. In all standard models the output of the neuron does not depend on time, as it is usually interpreted as the mean firing rate, a time averaged quantity. In our model the temporal information is taken into account by using spiking neurons, and by using time dependent mechanisms for synaptic plasticity.

## 2 Neuron models

Biological neurons output a series of action potentials (electrical pulses) in response to stimulation. These action potentials are the most relevant elements used in modeling neurons. Depending on the way they are described, the neuron models fit into one of two categories: firing rate models and spiking models. The most widely used model is the mean firing rate model (based on the average number of pulses emitted by a neuron in a time interval); it is also the simplest to describe in mathematical terms.

Networks of spiking neurons, on the other hand, must consider the spike forming mechanism, the methods of transmission, and the interactions between the spikes, which make them more difficult to describe.

There are many other elements of biological relevance such as the compartmental geometry or the channel variables involved at the synapse. The inclusion of all these elements would make networks of such neurons extremely difficult to simulate on serial machines.

### 2.1 Firing rate models

Neurons driven by a stimulus usually emit action potentials, which carry the signal along the axon to the synapses on the dendritic tree of other neurons. By counting the number of action potentials emitted by a neuron in some time interval (typical time window ranges from 100 to over 1000 ms) and dividing it by the length of the interval, we find the mean firing rate of the neuron. The dependence of the mean firing rate  $y_i$  of neuron  $i$  on the value of its input  $x_j$  is called the activation function of the neuron. In standard approach to NNs the output from a postsynaptic neuron  $i$  is the weighted sum of the incoming activity through the activation function

$$y_i = f\left(\sum w_{ij} \cdot x_j\right) \quad (1)$$

where the sum runs over all neurons which are presynaptic to neuron  $i$ . The coefficient  $w_{ij}$  denotes the synaptic efficacy of the synapse between  $j$  and  $i$  and is adjusted by some learning rule. Usually, the activation function  $f(\cdot)$  is either a threshold function or a sigmoid. Equation (1) defines the rate model of neural activity as used in most standard approaches.

Time dimension can be added to firing rate model described by Equation (1). One approach is to discretize the time and interpret Equation (1) as a mapping from one time step to the next [5]

$$y_i(t+1) = f(\sum w_{ij} \cdot x_j(t)) \quad (2)$$

$$\tau \frac{dy_i}{dt} = -y_i + f(\sum w_{ij} \cdot x_j) \quad (3)$$

Another possibility is to turn Equation (1) into a differential equation by introducing a time constant  $\tau$  [5]

The time constant  $\tau$  can be interpreted as a membrane parameter  $\tau=RC$  where  $R$  and  $C$  are the resistance and capacitance of the neuron.

## 2.2 Spiking models

The next step in modeling of biological neuron is to consider the fact that communication among neurons takes place through spikes. The spiking neurons are characterized by a membrane potential  $E$  and a threshold  $T_h$ . When the membrane potential reaches the threshold, an action potential (spike) is produced. Membrane potential dynamics and spike transmission description give rise to different models.

In biological neurons a spike is generated by a strong depolarization of the membrane potential when it reaches the threshold. Immediately after the generation of a spike the neuron cannot respond to any stimulation for a short period of time called *absolute refractory period*, and then only to a very strong stimulation, for another time interval called *relative refractory period*, during which the potential rebounds. Once a spike is generated it travels along the axon and, at the synapse locations, a postsynaptic potential (with either excitatory or inhibitory effect) is transmitted to the postsynaptic neuron. These postsynaptic potentials are then spatio-temporally integrated and they affect the postsynaptic neuron membrane potential.

In the currently used models, the *postsynaptic potentials* (PSP) are described in different ways but regardless of the model used a synaptic efficacy (weight) is always associated with each synapse. These weights are considered to be plastic, and the process of learning is associated with their modifiability. The simplest PSP is described as a delta function

$$PSP(t, t_i) = \delta(t - t_i) \quad (4a)$$

where  $t_i$  is the time of firing of presynaptic neuron. The effect is an instant jump in the membrane potential of the postsynaptic neuron. The next representation is that of a decaying exponential

$$PSP(t, t_i) = \exp(-\frac{t - t_i}{\tau}) \quad (4b)$$

where  $\tau$  is a time constant. More realistic models include the alpha function [1]

$$PSP(t, t_i) = \frac{t - t_i}{\tau} \cdot \exp(-\frac{t - t_i}{\tau}) \quad (4c)$$

and the double exponential function [1]

$$PSP(t, t_i) = \frac{\tau_r \tau_f}{\tau_r - \tau_f} \cdot \left[ \exp(-\frac{t - t_i}{\tau_r}) - \exp(-\frac{t - t_i}{\tau_f}) \right] \quad (4d) \quad 3$$

Computer generated representations of these postsynaptic potential models are illustrated in Figure 1.

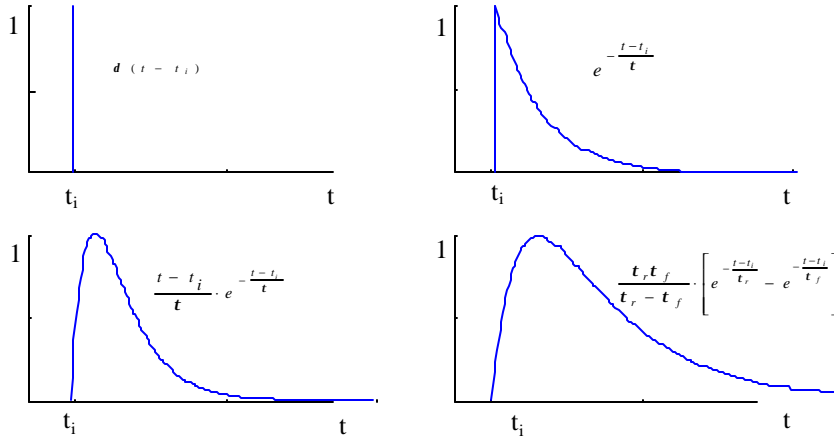


**Figure 1.** Normalized PSPs.

### 2.2.1 Integrate and fire models

Firing rate models assume that all relevant information is contained in the mean firing rate. In networks of spiking neurons we consider single spikes of single neurons as the essential information.

In the integrate and fire model, the neuron is described as a leaky integrator that fires, if the membrane potential  $E(t)$  reaches a threshold  $T_h > 0$ . After firing the membrane potential is reset to its initial value  $E(t_0)$ . Between two spikes the change of the membrane potential is described by the differential equation of an RC circuit

$$t \frac{dE}{dt} = -E + R (I^{syn} + I^{ext}) \quad (5)$$

where  $t=RC$  is the membrane time constant of a neuron with resistance  $R$  and capacitance  $C$ . The currents  $I^{syn}$  and  $I^{ext}$  describe the synaptic and respectively external input. The synaptic input for neuron  $i$  is given by the equation

$$I_i^{syn}(t) = \sum w_{ij} \cdot PSP(t, t_j) \quad (6)$$

where the sum is taken over all neurons which are presynaptic to neuron  $i$ ,  $w_{ij}$  is the synaptic efficacy of the synapse between neuron  $j$  and neuron  $i$ , and  $t_j$  denotes the firing time of neuron  $j$ .

The standard description of the integrate-and-fire model is the linear differential equation (5). It describes the dynamics in an RC circuit with constant  $t=RC$ . In real neurons both  $R$  and  $C$  have an intricate voltage dependence, since ion channels open and close as a function of the membrane voltage and/or the ion concentration.

### 2.2.2 Ion channel model

Another category is represented by models based on the description of ionic mechanisms similar to the one employed by Hodgkin and Huxley [6], and underlying the initiation and propagation of action potentials in the squid giant axon. The

membrane model is based on the equivalent electrical circuit of Figure 2. Writing the current flow equilibrium equation we obtain:

$$C \frac{dE}{dt} = -g_l(E - E_l) - g_K(E - E_K) - g_{Na}(E - E_{Na}) \quad (7)$$

where  $g_l$  is the leak conductance,  $g_K$  and  $g_{Na}$  are the active (voltage dependent) potassium and sodium conductances, and  $C$  is the membrane capacity. The potentials  $E_l$ ,  $E_K$ , and  $E_{Na}$  represent the reversal potentials of the respective ionic currents. Actually, Hodgkin and Huxley determined a formula to calculate  $g_K$  and  $g_{Na}$  based on experimentally measured values.

If we add to the previous equation an external current and/or a synaptic

current we get a simplified neuron description. More elaborate models take into consideration the dendritic tree, the soma, and the axon individually. Thus, the models become more accurate but at the same time more complex and harder to simulate in networks comprised such neurons.

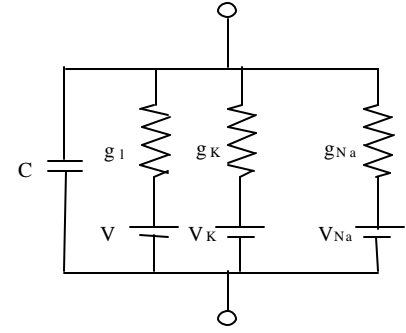


**Figure 2.** Membrane equivalent circuit

## 3 Neural network model

### 3.1 Spiking neuron

The neuron model that we chose for our NN is somewhere in between the integrate and fire model and the ion channel model. We use as a computational unit a modified version of MacGregor' spiking neuron model [11, 12]. The properties of the spiking neuron are defined by four state equations. These are equations for transmembrane potential generator, refractory properties, threshold accommodation, and a spiking variable

$$\begin{aligned} \frac{dE}{dt} &= \frac{-E + (SC + G_k \cdot (E_k - E) + G_i \cdot (E_i - E) + G_e \cdot (E_e - E))}{T_{mem}} \\ \frac{dT_h}{dt} &= \frac{-(T_h - T_{h0}) + C * E}{T_{th}} \\ \frac{dG_k}{dt} &= \frac{-G_k + B * S}{T_{gk}} \\ S &= \begin{cases} 1 & \text{if } E \geq T_h \\ 0 & \text{otherwise} \end{cases} \end{aligned} \quad (8)$$

Here  $E$  is the transmembrane potential,  $T_h$  is the time-varying threshold,  $G_k$  is the potassium conductance,  $SC$  is the external current input,  $E_k$  is the membrane resting potential,  $G_i$  and  $G_e$  are the synaptic conductances,  $E_i$  and  $E_e$  are the synaptic resting potentials,  $T_{mem}$  is the membrane time constant,  $T_{h0}$  is the resting value of the threshold, parameter  $C \in [0,1]$  determines the rise of the threshold,  $T_{th}$  is the time constant of decay of the threshold, parameter  $B$  determines the amount of the postfiring potassium increment,  $T_{gk}$  is the time constant of decay of  $G_k$  and  $S$  is the spiking variable, which takes the

value 1 when the cell fires and 0 otherwise. In the model individual EPSPs and IPSPs that result from changes in the synaptic conductances are modeled by alpha functions with different time constants  $T_e$  and  $T_i$

$$\begin{aligned} g_e(t) &= k \cdot \frac{t}{T_e} \cdot \exp\left(-\frac{t}{T_e}\right) \\ g_i(t) &= k \cdot \frac{t}{T_i} \cdot \exp\left(-\frac{t}{T_i}\right) \end{aligned} \quad (9)$$

Here  $k$  is a normalizing constant equal to  $e$  (the natural logarithm base).

Summing the contributions of all EPSPs and IPSPs at time  $t$  we obtain the total excitatory and inhibitory synaptic conductance changes

$$\begin{aligned} G_e(t) &= \sum_{k \in V_e} w_{ek} \cdot g_{ek}(t) \\ G_i(t) &= \sum_{l \in V_i} w_{il} \cdot g_{il}(t) \end{aligned} \quad (10)$$

where  $w_e$  and  $w_i$  are the excitatory and inhibitory synaptic efficacies (weights), and  $V_e$  and  $V_i$  are the sets of excitatory and inhibitory presynaptic neurons. The fact that excitation and inhibition are mediated through different neurotransmitters and receptors allows us to model the EPSPs and IPSPs with different time constants and also explains why the resting potentials for the two types of synapses are different.

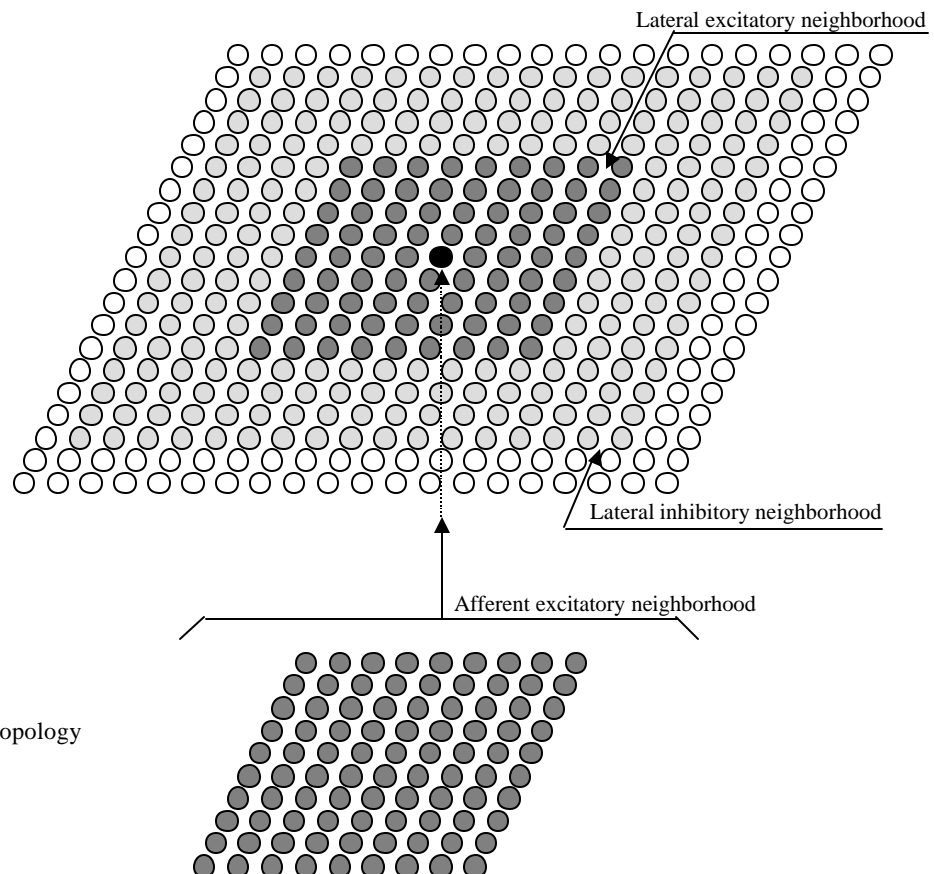


**Figure 3** The model topology

### 3.2 Network topology

The network model consists of two layers of interconnected neurons: an input layer that corresponds to receptors, and a cortical layer. Stimulation is conveyed to the cortical layer through a 2-dimensional input layer of receptor neurons. The role of these neurons is to transform the stimuli presented as input currents into spikes that are further relayed to the cortical layer [14].

The cortical layer is also organized as a 2-dimensional (19x19) array of neurons. Within this layer the neurons are laterally connected through excitatory and inhibitory connections. The architecture of the network is shown in Figure 3.

### 3.3 Synaptic plasticity

The weight adaptation process is activity dependent and instantaneous. The first rule we propose is a direct adaptation of the Hebbian rule with normalization used in the firing-rate models  $w_{k+1} = (w_k + \alpha y x) / \|w_{k+1}\|$ . Here the modification of the weight at iteration  $k+1$  is proportional to the dot product of the activity of the neuron described by its output  $y$ , and the input  $x$  representing the output activity of the projecting neurons. In our approach the activity is not described any longer by the average number of spikes but by single spikes and by the PSPs they transmit to other neurons. Therefore, instead of  $x$  we consider the sum of all PSPs projected onto the neuron, and  $y$  becomes the spiking variable  $S$  from Equations (8). Modification of the weights of a neuron takes place every time it fires ( $S = 1$ ). The afferent input weights and both the excitatory and inhibitory lateral weights are modified according to the same rule

$$w_{ij}(t+1) = \frac{w_{ij}(t) + \alpha \cdot g_{ij}(t)}{\sum_{j \in V_i} (w_{ij}(t) + \alpha \cdot g_{ij}(t))} \quad (11)$$

where  $g_{ij}$  is the post synaptic potential at the synapse between neuron  $j$  and  $i$  at the time of firing, expressed as a conductance change as in Equation (9),  $\alpha$  is the learning rate and  $V_i$  is the presynaptic vicinity. This type of adjustment, which will be further referred to as *modified Hebb's rule* strengthens the correlated activity and then distributes the changes through normalization. It depends on the temporal order [2], respecting causality and at the same time it quantifies this cause-effect relationship.

The other type of synaptic plasticity we propose is also implemented as Hebbian type learning. More precisely, whenever a neuron fires the connection strengths of all presynaptic neurons that excited it are modified according to the formula

$$w_{ij}(t+1) = \frac{w_{ij}(t)(1 + \alpha \cdot c_{corr})}{\sum_j (w_{ij}(t)(1 + \alpha \cdot c_{corr}))} \quad (12)$$

where  $w_{ij}(t)$  is the synaptic efficacy from neuron  $j$  to  $i$ ,  $\alpha$  is the learning rate, and  $c_{corr}$  is the correlation value. The correlation is given by

$$c_{corr} = (1 + y) \exp\left(-k \frac{t_j^2}{t_{corr}^2}\right) - y \quad (13)$$

Here  $t_j$  is the time passed since the last firing of neuron  $j$  ( $t_i=0$ ),  $y$  is the maximum value for the decay and  $k=\ln(1+1/y)$  is a scalar which assures that the zero crossing of  $c_{corr}$  takes place at  $t_{corr}$ . We will refer to this rule as *the temporal correlation rule*. Fig. 4 shows the dependence of  $c_{corr}$  on time, for  $y=0.5$  and  $t_{corr}=5$  ms. Figure 4 shows that if the

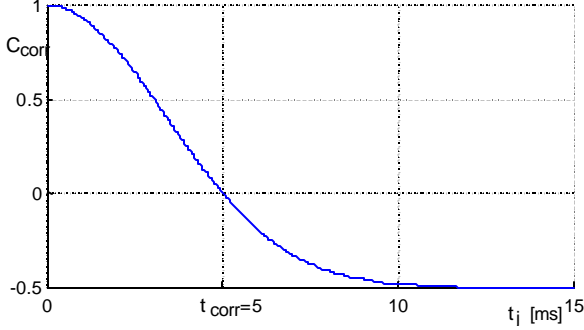


**Figure 4** Correlation value  $c_{corr}$  for  $t_{corr}=5$  ms and  $y=0.5$

correlation value is positive, the synaptic efficacy increases and if it is negative, the synaptic efficacy decreases. This type of dependence has some experimental basis [13]. A simple example can better explain the process. In Figure 5(a) we consider three neurons: two presynaptic ( $j$  and  $k$ ) and one postsynaptic ( $i$ ). Figure 5(b) shows their activity. Resetting to zero their time reference indicates the time of firing for each neuron. At  $t_i=0$  neuron  $i$  fires. On the horizontal axis a thick line indicates  $t_{corr}$ , the interval (in our case 5 ms) for which presynaptic neurons firings would increase the synaptic strength. In the example shown presynaptic neuron  $j$  fired 2 msec earlier ( $t_j=2$ ) within the positive correlation interval, and thus it increases its strength with neuron  $i$ . The smaller the time difference, the bigger the increase. If the firing is

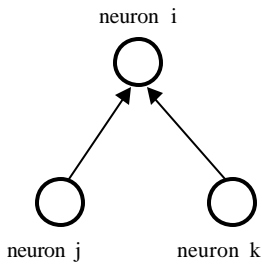
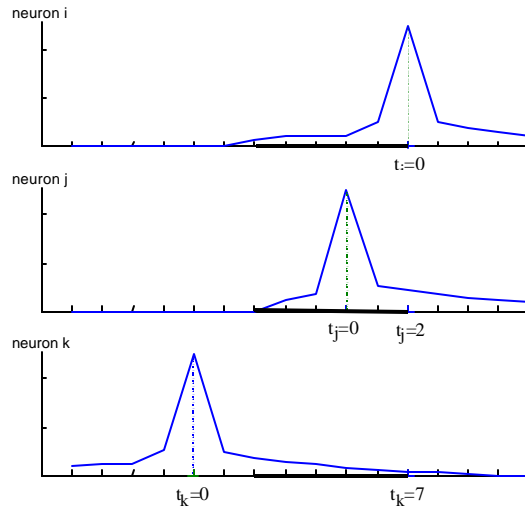


**Figure 5.** A three neuron circuit exemplifying the synaptic plasticity (a) the circuit (b) the activity of the neurons.



outside the interval the neuron decreases its strength, which is the case of neuron  $k$ . If the firing occurs close to the interval the decrease is smaller. This rule is competitive as neurons that fire within a time interval are rewarded and the other neurons are penalized. Note also that the rule is time order dependent. For two neurons, pre- and postsynaptically



connected to each other, the order of spiking is essential since one connection will be strengthened and the other will be weakened depending on which neuron fires first. This type of synaptic plasticity can be employed for all four PSPs representations, whereas the modified Hebb rule cannot work using the function described by Equation (4a).

One of the problems encountered in networks of spiking neurons is the initial value of the connection weights. There is a relationship between the initial receptive field dimension and the weights initialization in case of normalization. The bigger the receptive field area the smaller the weights and bigger the number of relatively synchronized presynaptic neurons firings necessary for triggering activity in the postsynaptic neuron. We addressed this problem by randomly choosing the weights within 25% of the uniform value  $1/n$ ,  $n$  being the total number of neurons in the receptive field. In addition, when changing the dimension of the receptive field, we modify the normalizing constant so that the influence of a neuron remains similar.

## 4 Experiments

Our basic experiment consists of showing how the receptive fields and weights of neurons change in response to input activity. Input signal was taken to be of Gaussian shape, with values above the threshold necessary to trigger firings in the stimulated neuron. The input neurons were stimulated directly using external current given by the SC term in Equation

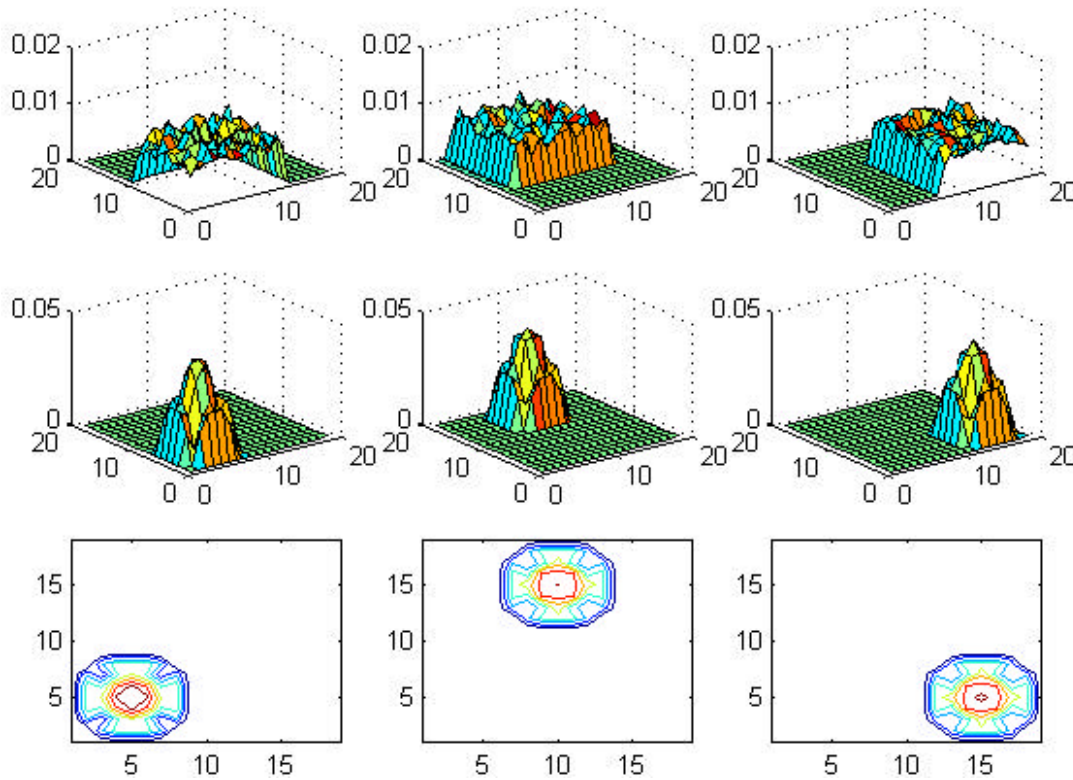


**Figure 6.** Receptive fields of neurons (4,7), (14,9) and (7,14) from the three formed regions.  
Top row: initial weights; Middle row: final values ; Bottom row: contour plots of final values

(8). The values of the parameters used in the simulation are given in the Appendix. The stimulated neuron responds with an increased firing frequency to increasing values in the SC term, but the relationship is not linear. Three regions of the input array were stimulated with the same Gaussian-shaped signal. The network was stimulated for a total of 3000 cycles. Each cycle consisted of random presentation of the input signal to one of the three chosen regions for a period of 100 msec followed by a cool-off period of another 100 msec, for a total of 200 msec per cycle. The cool-off period served two purposes: to check that the network still worked in the stability region, and at the same time to allow for latent activity even after the stimulation was removed. At each time step the afferent, lateral excitatory and lateral inhibitory connection weights were adjusted according to Equation (11). Below we analyze what happened in each case.

*Afferent connections.* Initially, the "cortex" neurons have an afferent receptive field somewhere between  $7 \times 7$  and  $13 \times 13$ , depending on how close to the edge of the array they are. During the process each neuron gradually adjusts its afferent weights towards the active neurons in the input layer. As a result the top layer was divided into three regions. Figure 6 shows the afferent weights profile of three neurons, one of each region. This process was expected for neurons with initial afferent receptive field overlapping only one stimulated region. But there were many neurons with afferent receptive field overlapping two or even all three stimulated regions that eventually developed a preference toward one region only. In this case the lateral connections have an important role, but the number of consecutive stimulations of the same input was not a factor. We made sure that every three cycles all input regions were stimulated, which means that an input region cannot be stimulated more than two times in a row.

*Lateral connections.* The lateral connections started out with receptive fields between  $5 \times 5$  and  $9 \times 9$  for excitatory connections and the entire cortical layer of  $19 \times 19$  neurons for the inhibitory connections. Both types of connections

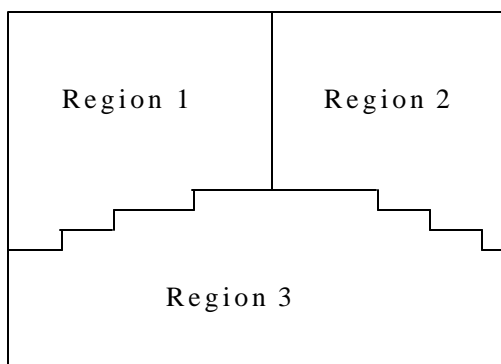


**Figure 7.** The three regions map obtained by using Equation (11) as learning rule

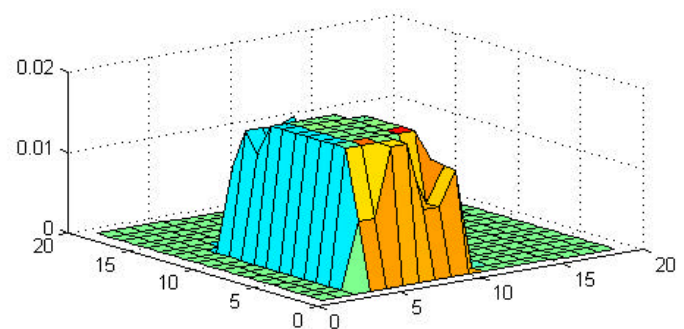


**Figure 8.** Lateral excitatory connection of neuron (8,10)

gradually restricted their influence to neurons within one region only. Thus, depending on their initial spread, they were completely confined to one region or another. The complete separation in the three regions is shown in Figure 7.

The lateral connection weights became relatively equal as shown in Figure 8. This was due to the fact that close neurons within the same region acquired almost identical afferent connections and, as a result their activity became similar. Next, we analyzed the same network using the temporal correlation rule. For a better comparison between the two cases, we started out with the same initial connection weights and followed the same order of presentation of inputs. Interestingly, the behavior was very similar. The afferent connections gradually restricted their area slightly more than before and their profile was smoother, as shown in Figure 9. Similarly, the lateral connections confined themselves into the newly formed areas. Figure 10 depicts the three regions formed. Taking a closer look at the map formation process we can make the following comments. From the shape of the  $c_{\text{corr}}$  function we see that for positive values, the smaller the time difference between the spikes of two connected neurons the more the increase in the synaptic weight, which, in turn will make the time difference even smaller next time. We can state that the objective of this rule is to minimize the time difference between the spikes. Minimizing the time difference means synchronizing the activity of the neurons. In other words the rule synchronizes the activity of neurons. Under this interpretation we can go even further and state that  $t_{\text{corr}}$  defines the capture zone within which the neurons can acquire synchrony. This could make this temporal correlation rule a possibility for applications in pulse coupled neural networks [8].

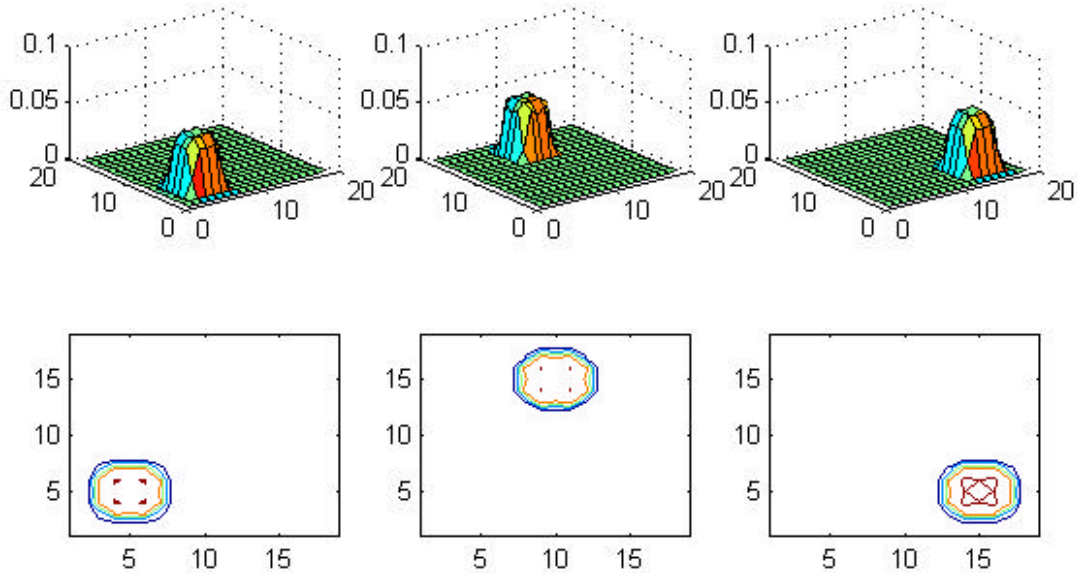


**Figure 9.** The profiles of the same three neurons presented in Figure 6 obtained by using the temporal correlation learning rule of Equation 12

An interesting analogy can be made between the learning rule as used in the Kohonen's Self-Organizing Map (SOM) network and our temporal correlation rule. Kohonen introduced a neighborhood function to define spatial relationship between neurons. Let us recall that the SOM network has no lateral connections. Kohonen's topological neighborhood function is usually defined in terms of the radius surrounding the winning neuron. The learning starts with a large radius value and decreases with the number of iterations. In our own rule we can define  $c_{\text{cor}}$  as a temporal neighborhood function with  $t_{\text{corr}}$  as the temporal radius. Under this interpretation we can consider  $t_{\text{corr}}$  as a time function. Then the learning process would start with a large temporal radius and as the learning proceeds this temporal radius decreases.

**Figure 10.** The three regions map obtained by using the temporal correlation rule

## 5 Conclusions

## Appendix

### Simulation parameters

Dimensions of the layers:	- input layer	19x19 neurons
	- "cortex" layer	19x19 neurons
The initial connection range:	- afferent	= radius of 6
	- lateral excitatory	= radius of 6
	- lateral inhibitory	= radius of 12
Correlation time:	- $t_{\text{corr}}$	= 10 msec

For the spiking neuron the following values were used in simulations; in parentheses the typical range is given.

$C = 0$ (and 0.6)	(0...1)
$B = 20$	(2...30)
$T_{\text{mem}} = 25$ msec	(5...30)
$T_{\text{gk}} = 3$ msec	(0.5...10)
$T_{\text{th}} = 25$ msec	(10...40)
$T_{\text{io}} = 10$ mV	(5...20)
$E_{\text{k}} = -10$ mV	(-20...-5)
$E_{\text{i}} = -10$ mV	(-20...-5)
$E_{\text{e}} = 70$ mV	(50...80)
$T_{\text{i}} = 2$ msec	
$T_{\text{e}} = 10$ msec	

## References

- [1] Arbib, M.A., Erdi, P., and Szentagothai, J., Neural Organization: structure, function, and dynamics, MIT Press, 1998.
- [2] Bell, C.C., Han, V.Z., Sugawara, Y., and Grant, K., "Synaptic plasticity in a cerebellum-like structure depends on temporal order", Nature, vol. 387, pp. 278-281, 1997.
- [3] Bialek, W. and Rieke, F., "Reliability and information transmission in spiking neurons", Trends in Neuroscience, vol. 15, pp. 428-434, 1992.
- [4] Gerstner, W. and van Hemmen, J.L., "How to describe neuronal activity: spikes, rates or assemblies?", Advances in Neural Information Processing Systems, vol. 6, pp. 463-470, Morgan Kaufmann, 1994.
- [5] Gerstner, W., "Time structure of the activity in neural network models", Physical Review E, vol. 51, pp. 738-758, 1995.

- [6] Hodgkin, A.L. and Huxley, A.F., "A quantitative description of membrane current and its application to conduction and excitation in nerve", *Journal of Physiology (London)*, 117, pp 500-544, 1952.
- [7] Hopfield, J.J., "Pattern recognition computation using action potential timing for stimulus representation", *Nature*, vol. 376, pp. 33-36, 1995.
- [8] Johnson, J.L., "Pulse-coupled neural nets: translation, rotation, scale, distortion, and intensity signal invariance for images", *Applied Optics*, vol 33, pp. 6239-6253, 1994.
- [9] Judd, K.T. and Aihara, K., "Pulse Propagation Networks: A Neural Network Model That Uses Temporal Coding by Action Potentials", *Neural Networks*, Vol. 6, pp. 203-215, 1993.
- [10] Kohonen, T., *Self-Organizing Maps*, Springer, 1995.
- [11] MacGregor, R.J., *Neural and Brain Modeling*, Academic Press, 1987.
- [12] MacGregor, R.J., *Theoretical Mechanics of Biological Neural Networks*, Academic Press, 1993.
- [13] Markram, H. and Tsodyks, M., "Redistribution of synaptic efficacy between neocortical pyramidal neurons", *Nature*, vol. 382, pp. 807-810, 1996.
- [14] Sala, D.M., Cios, K.J., and Wall, J.T., "A Spatio-Temporal Computer Model of Dynamic Organization Properties of the Adult Primate Somatosensory System", *Progress in Connectionist-Based Information Systems, Proc. of the 1997 Intl. Conf on Neural Information Processing and Intelligent information Systems*, Springer, vol.1, pp. 153-156.
- [15] Sejnowski, T.J., "Time for a new neural code?", *Nature*, vol. 376, pp. 21-22, 1995.
- [16] Shepherd, G.M., *Neurobiology*, 3<sup>rd</sup> ed., Oxford University Press, 1994.
- [17] Thorpe S.J. and Imbert, M., Biological constraints in connectionist modeling, In: *Connectionism in Perspective*, Eds. R. Pfeifer, Z. Schreter, F. Fogelman-Soulie, and L. Steels, Elsevier, North Holland, 1989.